AE 512 Final Project Part 1

Alexander Wang

November 27, 2024

1 Comparative Analysis

1.1 Velocity

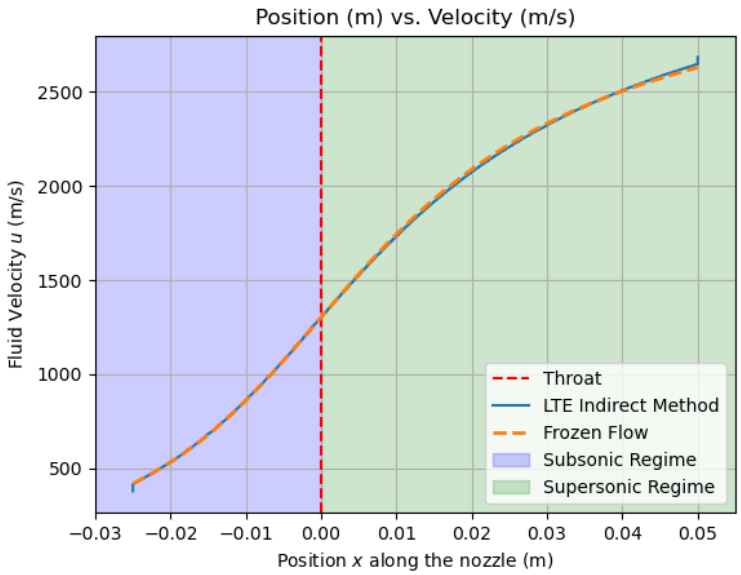

Figure 1: Graph of the velocity of the fluid along the x-direction of the nozzle.

Both the LTE approach and the frozen flow approach have similar, increasing profiles. This is because enthalpy decreases along the nozzle, so velocity is expected to increase. Supposedly the velocity transitions should be smoother for the LTE method due to the fluctuating thermodynamic properties. The velocity in the supersonic regime also goes slightly lower than the frozen flow (ignoring the ends blowing up due to being out of interpolation range). This is because energy is being absorbed in vibrational/rotational modes of the gas, whereas with frozen flow all energy is kinetic energy.

1.2 Pressure

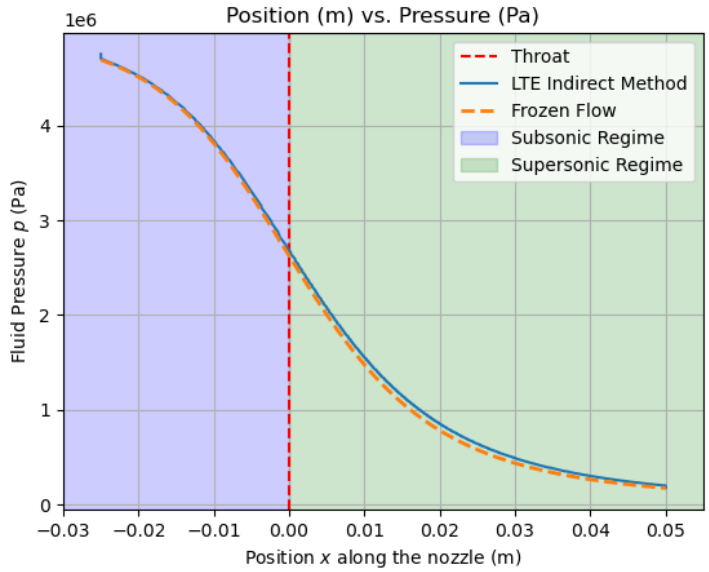

Figure 2: Graph of the pressure of the fluid along the x-direction of the nozzle.

The LTE approach produced a more linear and gradual decline across the throat from the subsonic to the supersonic regime. This can be attributed to the internal energy modes slowing down flow acceleration. On the other hand, with frozen flow, pressure drops slightly more sharply, because frozen flow ignores energy loss while having a higher flow velocity.

1.3 Temperature

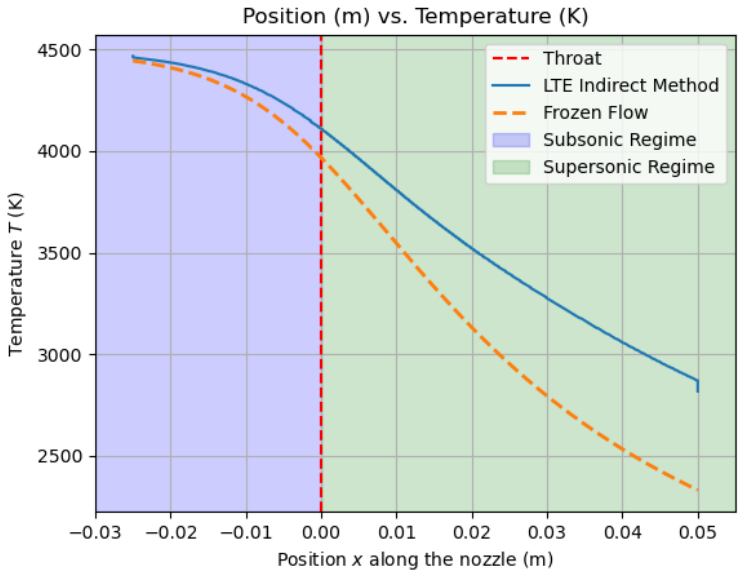

Figure 3: Graph of the temperature of the fluid along the x-direction of the nozzle.

The LTE temperature decreases more gradually. Similar to pressure, this is because energy is absored into internal energy modes. LTE accounts for resistive molecular processes that resist temperature

changes. Frozen flow has a sharper drop. This is because all energy is attributed to translational kinetic energy, ignoring the resistive processes in LTE.

1.4 Density

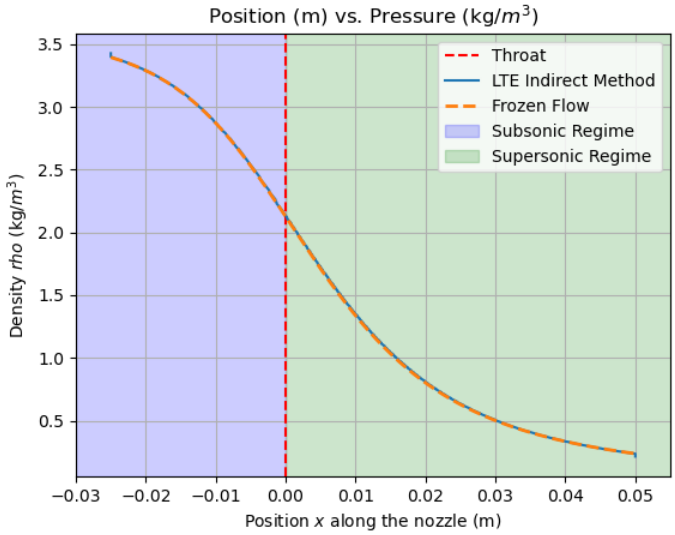

Figure 4: Graph of the density of the fluid along the x-direction of the nozzle.

The LTE approach and the frozen flow approach show similar results. This can be attributed to the initial reservoir conditions we chose. Supposedly, density should decrease more gradually downstream of the throat compared to frozen flow, reflecting energy absorbed into internal energy modes. This is only slightly evident in the graph.

1.5 Mach Number

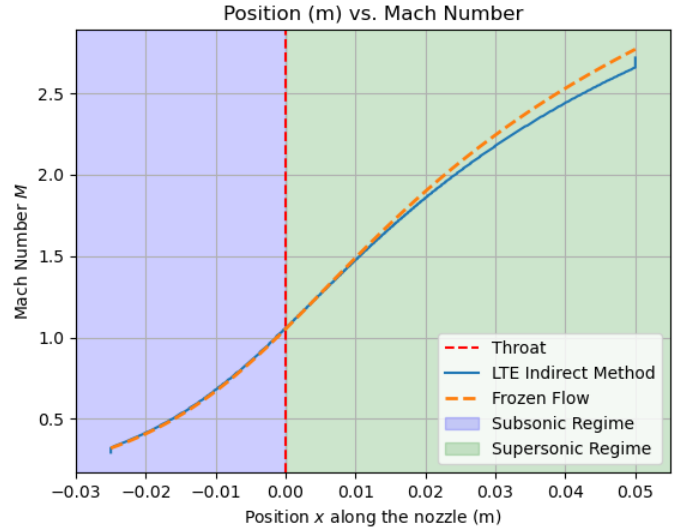

Figure 5: Graph of the Mach number of the fluid along the x-direction of the nozzle.

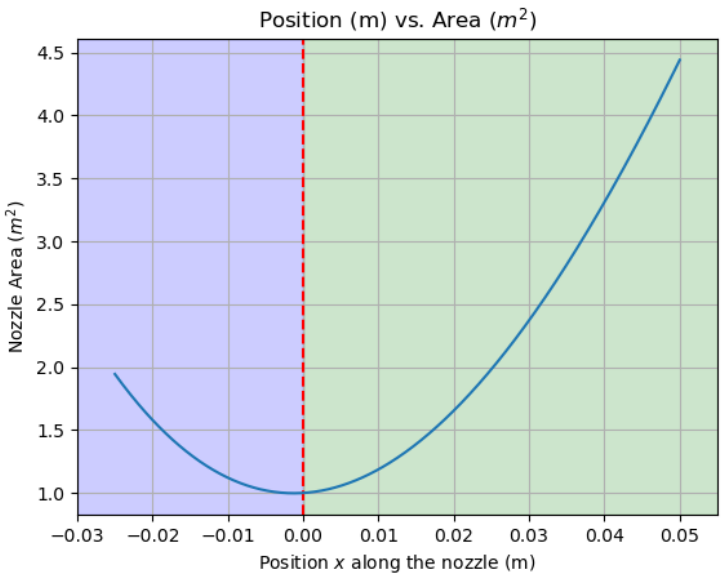

Figure 6: Graph of the cross-sectional area of the nozzle along the x-direction.

The mach number follows an increasing trend similar to velocity. This is because Mach number is related to fluid velocity. With the frozen flow model, the increase in Mach number is sharper past the throat in the supersonic regime, because at corresponding positions, velocity is higher and density is lower for the frozen flow model.

1.6 Regime Differences

Both models correctly predict Mach number at the throat. Both models also have similar behavior in the subsonic regime (besides temperature). In the supersonic regime, however, frozen flow has more dramatic changes, while the LTE approach features more gradual change. This is because the initial energy is absorbed into internal energy modes, which accumulate significantly past the throat of the nozzle. Since frozen flow doesn't account for this, it deviates more from LTE in the supersonic regime. This is due to frozen flow fixing specific heat. Thermodynamic properties such as specific heat change with different temperatures, particularly in high temperatures. By fixing thermodynamic properties, we don't account for the energy absorbed into the internal modes.

2 Appendix

2.1 Graphs

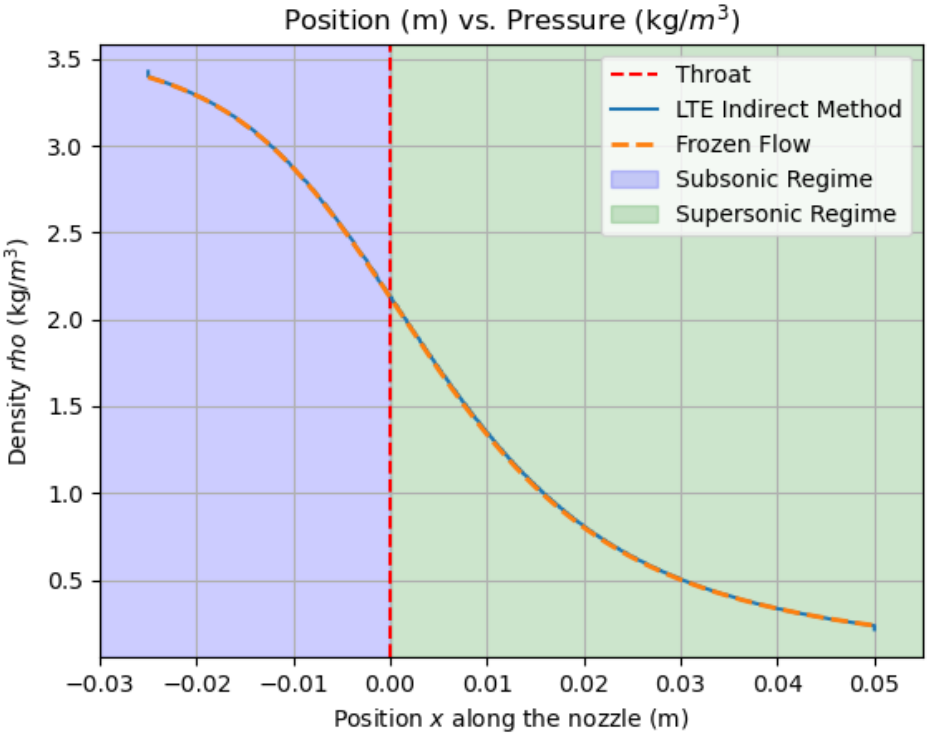

Figure 7: Graph of the density of the fluid along the x-direction of the nozzle.

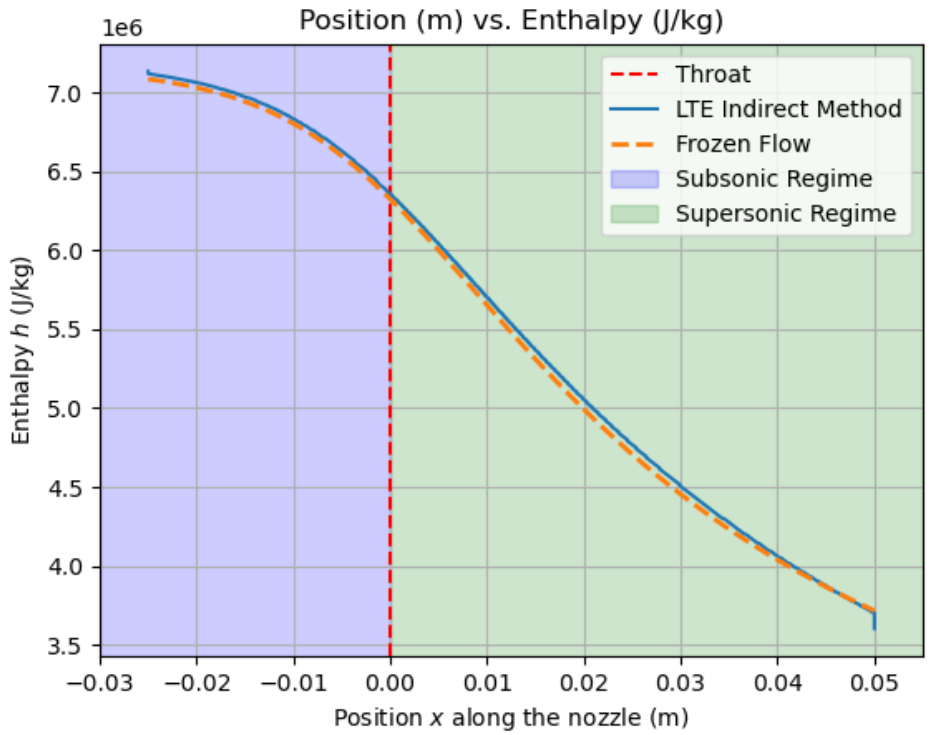

Figure 8: Graph of the enthalpy per unit mass of the fluid along the x-direction of the nozzle.

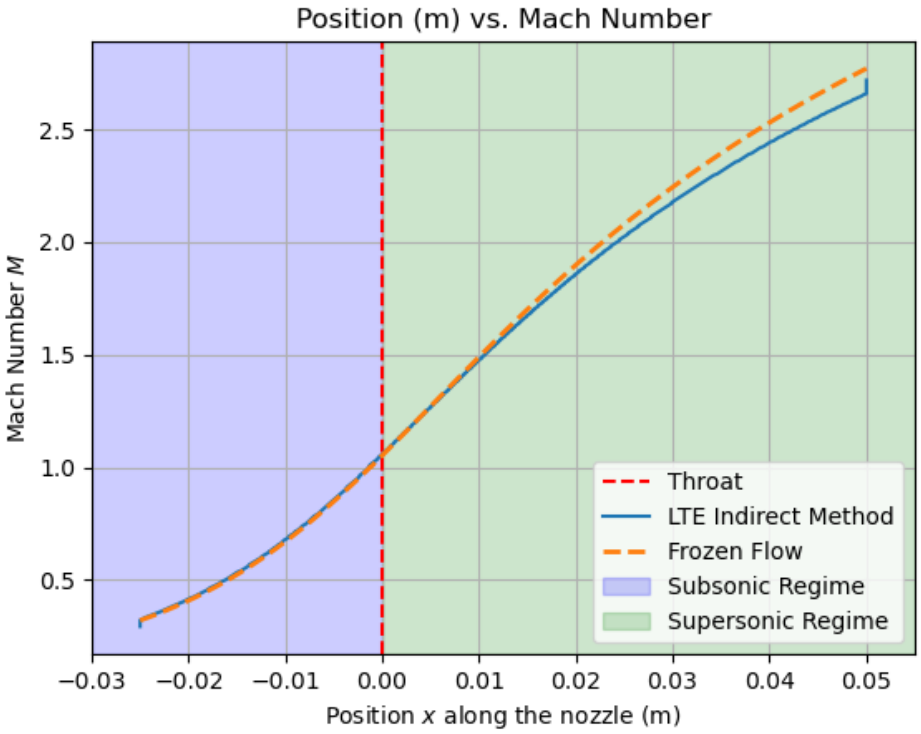

Figure 9: Graph of the Mach number of the fluid along the x-direction of the nozzle.

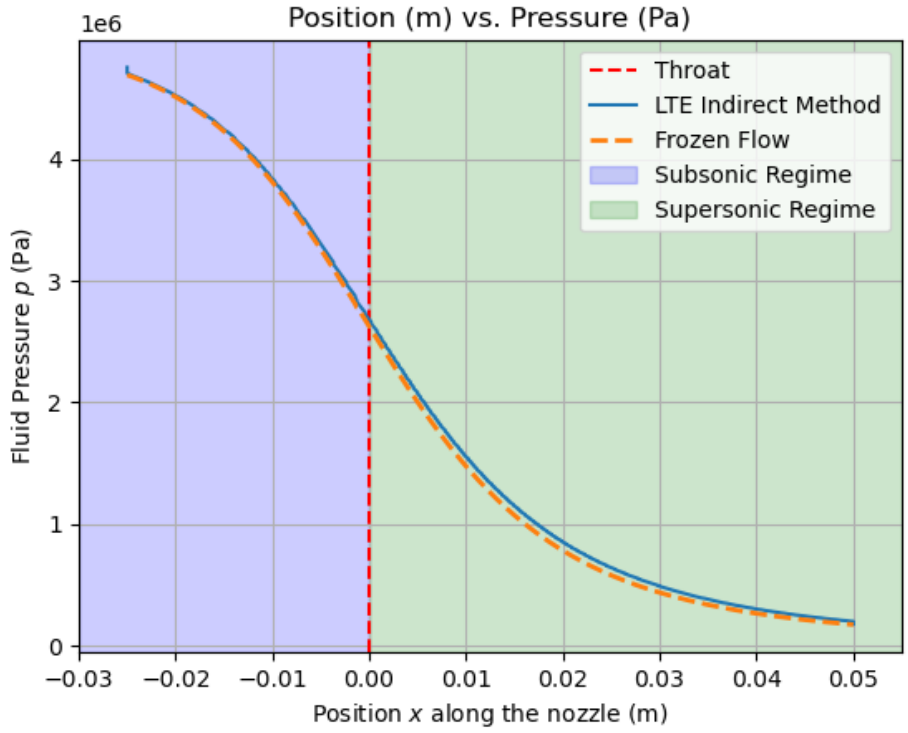

Figure 10: Graph of the pressure of the fluid along the x-direction of the nozzle.

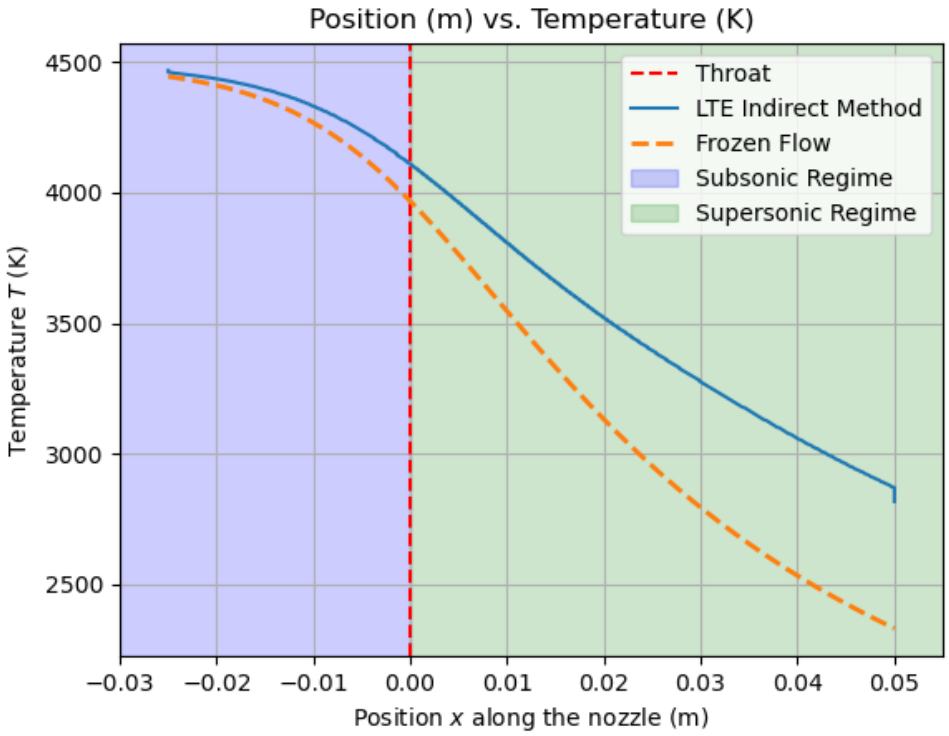

Figure 11: Graph of the temperature of the fluid along the x-direction of the nozzle.

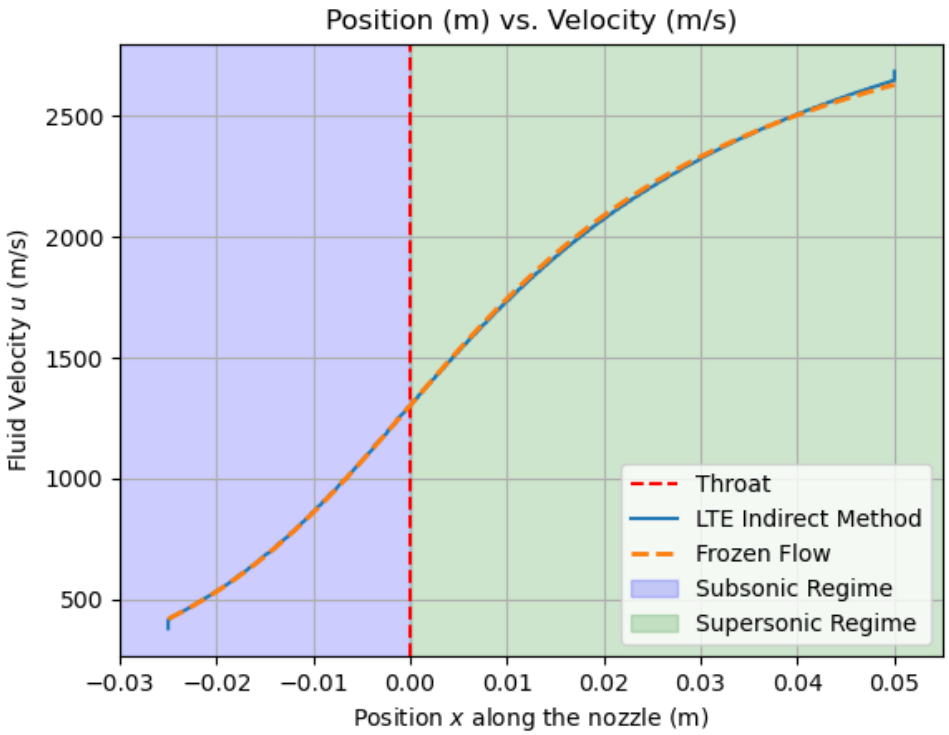

Figure 12: Graph of the velocity of the fluid along the x-direction of the nozzle.